12th International Conference on Applications of Statistics and Probability in Civil Engineering, ICASP12
Vancouver, Canada, July 12-15, 2015

Computational Simulation of Hydraulic Fracturing Nonlinear Dynamics using Gaussian Processes Surrogates

Souleymane. Zio
Phd Student, Dept. of Mechanical Engineering , Federal Univ. of, Rio de janeiro, Brazil

Fernando A. Rochinha
Professor, Dept. of Mechanical Engineering , Federal Univ. of, Rio de janeiro, Brazil

ABSTRACT: High-Fidelity physics based computational models enables the design and optimization of complex engineered processes. Moreover, important and strategic decisions might be taken relying on those computational models predictions. Therefore, there is a need for improving their robustness and reliability. Therefore, understanding the impacts on the predictions due to unavoidable input and model structures uncertainties, often referred to as Uncertainty Quantification (UQ), has become a major issue. A key aspect in this context is the demand of a significant computational effort involving many-queries of a computer code. That might be lessen by the use of reduced order models or any form of surrogates. Here, we employ Gaussian Processes (GPs) as a surrogate (often referred to as emulators) for a computer code devoted to Hydraulic Fracturing simulation.

1. INTRODUCTION

Hydraulic fracturing (HF) is a widely used engineering process in the petroleum industry for improving the productivity of the oil and gas reservoirs. The fracturing fluid is pumped into the well at an elevated pressure, this pressure must be greater than the minimum in-situ stress to create a fracture in the reservoir rock. The mathematical model of this process relies on complex nonlinear and free boundary problems leading to complex computer models. To resolve this free boundary and multi-scale problem, the implicit level set is combined with the plane asymptotic solutions at the tip of the fracture (Peirce, 2014). The solution at the tip depends on the different physical processes namely, storage viscosity, storage-toughness, leak-off viscosity and leak-off-toughness. Each of these processes has different values of the asymptotic solution at the tip of fracture which depends also of the reservoirs rock properties. Typically, the modeling of a HF involves scenarios that present uncertainties in the Geomechanics properties, like, for instance, but not limited to, Elasticity Modulus and confining stresses. In literature, several methods are used to take into account uncertainty over the parameters in the numerical simulation. Methods such as Monte Carlo (MC), general Polynomial Chaos(gPC) (Ghanem and Spanos, 1991), Multi-element generalized Polynomial Chaos(ME-gPC)(Xiaoliang Wan, 2005), stochastic collocation (Zio and Rochinha, 2012), Adaptive stochastic collocation (ASCM) present some difficulties related to computational demand, convergence, and to calculate some statistics information. One of the common aspects of these methods is the demand of a high computing effort involving many-requests from a computer code. That might be lessen by the use of reduced order models or any form of surrogates(often referred to as emulators)(, Mingjie Chen). Here, we employ a nonstationary Multivariate Gaussian process as surrogate(MGPs) (Bilionis and Zabaras, 2008) for a computer code devoted to Hydraulic Fracturing simulation. The MGPs constructs in this work can be efficient to approximate the nonlinear and nonsmooth behaviors of HF response in heterogeneous, discontinuous reservoir rock.

2. HYDRAULIC FRACTURE MODELING

Modeling the evolution of a hydraulic fracture in a geologic formation involves distinct physical processes: deformation of the surrounding elastic medium, the fracture propagation, the flow of a viscous fluid within the fracture, and the leak-off of the fracturing fluid. In order to achieve a balance between accuracy and easiness of the simulation, a number of reasonable simplified models, which are readily justifiable in the present context, are combined to describe the multiphysics scenario. The fracture grows in limit equilibrium, following the linear elastic fracture mechanics , within a layered formation portraying homogeneous layers (spatially uniform values of the toughness K_{ic} of the Elastic Modulus E and of the Poisson ratio ν). Assuming a plane strain state, the elastic problem, and consequently the flow problem, is reduced to a one dimensional spatial setting (Adachi and Detournay, 2008) with coordinate x coincident with the fracture propagation direction and occupying a domain that evolves with the time t described by the interval $\ell(t) = [l_{low}(t), l_{up}(t)]$. The fracture is propagated by the injection, through the well, of an incompressible Newtonian fluid with dynamic viscosity μ. As the flow takes place in the confined interior volume of the fracture delimited by its aperture $w(x,t)$, lubrication equation is assumed to model the flow behavior characterized by the pressure $p_f(x,t)$ and fluid flux $q(x,t)$. The whole process is controlled by the injection rate Q_0 and the physical and geological conditions imposed by the rock formation, namely: the confining stress σ, perpendicular to the fracture aperture direction, and the four material parameters E', μ', K', and C' defined as: $E' = \frac{E}{1-\nu^2}$; $\mu' = 12\mu$; $K' = 4(\frac{2}{\pi})^{\frac{1}{2}} K_{ic}$; $C' = 2C_l$. Here, E' is the plane strain modulus, μ' the alternate viscosity, C' the leak-off coefficient and K' the rock toughness.

The governing equations are presented below in a dimensionless form resulting from a scaling that allows to unveil the different fracture evolution regimes, which will not be discussed here due to the lack of space, but are pivotal in the design of the numerical approach proposed in (Peirce and Detourney, 2008). This scaling introduces characteristics length, time, pressure, and fracture opening: ℓ_*, t_*, w_*, p_*, to be determined in line with the aforementioned propagation regimes. Therefore, the quantities of interested are expressed as: $x = \ell_* \chi$,$t = t_* \tau$, $w = w_* \Omega$, $p_f = p_* \Pi_f$, $\sigma_0 = p_* \Sigma_0 \Phi(\chi)$, $Q = Q_0 \Psi(\tau)$. The quantities $\chi, \tau, \Omega, \Pi_f$ represent the dimensionless spatial coordinate, time, fracture aperture and fluid pressure. Moreover, $\Phi(\chi)$ is the spatial distribution of the confining stress.

Elasticity Equation

$$\Pi = \Pi_f(\chi,\tau,\varpi) - \Sigma_0(\varpi)\Phi(\chi,\varpi) = \frac{-G_E}{4\pi} \int_{-\ell_{low}(\tau,\varpi)}^{\ell_{up}(\tau,\varpi)} \frac{\Omega(\chi',\tau,\varpi)}{(\chi-\chi')} d\chi', \qquad (1)$$

where $\Pi(\chi,\tau,\varpi)$ stands for the nondimensional net pressure (resulting from the difference between fluid pressure and the geological confining stresses).

Lubrication Equation:

$$\frac{\partial \Omega}{\partial \tau} + G_c \frac{H(\tau - \tau 0(\chi))}{\sqrt{(\tau - \tau_0(\chi))}} = G_m \frac{\partial}{\partial \chi}[\Omega^3 \frac{\partial \Pi_f}{\partial \chi}] + G_v \Psi \delta_0(\chi), \qquad (2)$$

where H is the Heaviside function and δ_0 is the Dirac function centered at the injection points.

Boundary and Propagation Conditions:

$$\lim_{\xi \to 0} \Omega^3 \frac{\partial \Pi_f}{\partial \xi} = 0,$$
$$\Omega(\ell_{low,lup}, ., .) = 0, \qquad (3)$$

$$\lim_{\xi \to 0} \frac{\Omega}{\xi^{1/2}} = G_k, \qquad (4)$$

where $\xi = \ell(\tau, .) - \chi$ is a local coordinate representing the distance from a fracture interior point to the fracture tip. The first condition corresponds to no flux through the tips; the second implies that the fracture aperture vanishes, and the third one reflects the aperture asymptotic behavior corresponding to the linear fracture mechanics. The dimensionless quantities G_j above, whose values deter-

mine the propagation regimes, are defined as follows: $G_E = \frac{p_* \ell_*}{E' w_*}$, $G_m = \frac{\mu' Q_0}{w_*^3 p_*}$, $G_v = \frac{Q_0 t_*}{w_* \ell_*^2}$, $G_c = \frac{C' \ell_*^2}{Q_0 t_*^{1/2}}$, $G_k = \frac{K' \ell_*^{1/2}}{E' w_*}$.

Locating the free boundary using the tip asymptotics

Admitting $G_E = G_m = G_v = O(1)$, the above equations correspond to the viscosity dominate propagation regime (Peirce and Detourney, 2008), in which the viscous flow is the main dissipation mechanism, the tip fracture (within the spatial scale introduced by the numerical method) follows the asymptotic trend

$$\lim_{\xi \to 0} \Omega \sim \beta_{m0} V^{1/3} \xi^{2/3}, \tag{5}$$

where $\beta_{m0} = 2^{1/3} 3^{3/6} (\frac{\mu'}{E'})$, and V the normal velocity of the front, what is explored in the numerical scheme proposed in Peirce and Detourney (2008).

Besides the space and time coordinates χ and τ, we introduce above ϖ, a third argument for the fields above, in order to represent the random dimension needed for describing uncertainties in the input parameters within a probabilistic perspective. Here, we follow the same approach presented in (Zio and Rochinha, 2012)

3. NONSTATIONARY MULTI-OUTPUT GAUSSIAN PROCESSES (MGPS)

In this section, we briefly reproduce main concepts and building blocks proposed in Bilionis and Zabaras (2008) for developing local Gaussian surrogates considering multiple outputs and employing a Bayesian approach. The statistics of a Gaussian Process $\mathbf{f}(.)$ is completely specified through its mean and covariance functions. The first deals with the general trend of the random field and the covariance expresses the smoothness of the dependence on the arguments and the correlation between the different components.

In order to make the presentation simpler and more compact, we adopt a simplified formal notation, frequently found in the literature. The simulator (here corresponding to the numerical scheme used to solve the nonlinear partial differential equations presented in the previous section), is to be represented as a mapping connecting inputs $\mathbf{x}$ (material and control parameters, initial conditions,...) and outputs $\mathbf{y}$ (variables or quantities of interest like, for instance, fracture length and aperture, velocity of propagation), is denoted as $\mathbf{f}(\mathbf{x})$ with a K-dimensional input $\mathbf{x} \in \mathbf{X} \subset R^K$, i.e. $\mathbf{X} = \times_{k=1}^{\mathbf{K}} [a_k, b_k]$, $-\infty \leq a_k < b_k \leq \infty$. To reflect uncertainties in the input parameters, $\mathbf{x}$ is considered a random vector with probability density $p(\mathbf{x})$ defined as $\prod_{k=1}^{K} p_k(x_k)$, assuming independence between the individual inputs.

The multiple outputs of the simulator are organized in a vector form: $\mathbf{y} \in \mathbf{Y} \subset R^M$, where M represents the number of outputs. At this point, it is important to realize that the components of this vector might have different physical meanings (pressure, velocity or length), which requires normalization before the construction of the simulator surrogate. The simulator is ran at selected training inputs $\mathbf{X} = (\mathbf{x}^1, ..., \mathbf{x}^N)$, leading to the training outputs $\mathbf{Y} = (\mathbf{y}_r^1 = \mathbf{f}(\mathbf{x}^1), ..., \mathbf{y}_r^N = \mathbf{f}(\mathbf{x})^N)$ where $r = 1, .., M$. We assume that we have observed a fixed number $N \geq 1$ and training set $\mathbf{D} = \{(\mathbf{X}, \mathbf{Y})\}$.

From a Bayesian perspective, we regard $\mathbf{f}(.)$ as an unknown function to be inferred from the data produced at the training points. The motivation is to obtain a mapping $\mathbf{f}(.)$ which produces the simulator outputs at any inputs different from the training points efficiently. That means that we seek a significant reduction in the computational costs when compared with running the simulator itself. Therefore, we are seeking for replacing the original computational simulator that is referred to as a surrogate, many times also deemed as an emulator. As we are going to use limited data, the surrogate is at most only an approximation of the simulator, what, therefore, entails uncertainties in the desired predictions. This uncertainty in the outputs is not to be confused with the one induced by the parameters (inputs) of the model. We cast the uncertainty in a probabilistic framework and build the surrogate as statistical approximation of the deterministic simulator by combining a priori information with the data produced with the training. We consider as prior information that $\mathbf{f}(.)$ is a Gaussian Process (MGP) conditional on some hyper-

parameters. Baye's theorem and a gaussian likelihood function guarantees that the posterior distribution of $\mathbf{f}(.)$, regarded as a surrogate to the expensive computational simulator, is also Gaussian process conditional on the hyper-parameters, formally described by:

$$\mathbf{f}(.) \sim \mathbf{GP}(\mathbf{m}(\mathbf{x}), \mathbf{C}(\mathbf{x}, \mathbf{x'}; \Theta)), \tag{6}$$

where $\mathbf{m}(\mathbf{x})$ and $\mathbf{C}(\mathbf{x}, \mathbf{x'}; \Theta)$ are the mean and the covariance function of the GP and Θ the unknown hyper-parameters. The choice of covariance models for multiple outputs has been discussed in the literature, where one can find many different options. Here, we adopt the non isotropic Square Exponential function:

$$c_{SE}(\mathbf{x}, \mathbf{x'}) = s_f^2 \exp(-\frac{1}{2}\sum_{k=1}^{K}\frac{(x_k - x_k')^2}{\ell_k^2}), \tag{7}$$

In order to keep a compromise between accuracy and easiness on the use of a surrogate, we do not adopt a fully Bayesian approach. In that same line, all the outputs share the same correlation function, which does not allow an explicit modeling of the correlation between outputs. The hyper-parameters $\Theta = (s_f, \ell_1, ..., \ell_k)$, having as components the signal strength and the correlation lengths in each input direction, are obtained by maximizing the logarithm of the marginal likelihood. Here, we use the Conjugate Gradient method(CG) to maximize the log-likelihood, obtaining the optimal value Θ^*. Using the correlation function defined with Θ^* and the low order statistics (mean and variance) of the training data, we compute a GP surrogate and, therefore, we are able to make predictions at any input points.

Having this surrogate, we can address an Uncertainty Quantification study. We can compute the statistics of outputs such as mean, variance, and the probability distribution(PDF) due to uncertainties in the input parameters. That can be done either by sampling or, if possible, by computing the corresponding integrals analytically. Moreover, the uncertainty on those predictions due to the limited information used in the construction of the surrogate can be estimated by the final variance of the MGP. Here, we employ the adaptive strategy designed in Bilionis and Zabaras (2008) that explores this variance to guide the decomposition of the input space into disjoint subsets. For each subset, a local MGP is built to capture the evolving dynamics of the fracture as we use time dependent outputs. In the next section, along the numerical examples, the nature and choice of outuputs will be presented in further detail in the next section. A broader discussion of emulators to be employed as surrogates for simulators of dynamical systems lies outside the scope of this work and can be found in Stefano Conti (2010). Moreover, the adaptivity process also resorts, if needed, to the inclusion of more training points within a subdomain (until a prescribed number) such that an a priori accuracy threshold δ for the variance of the MGP is achieved. Technical details about the algorithm in its implementation can be found in Bilionis and Zabaras (2008) At the end of this adaptive process, the whole input space is covered with local approximations, which allows to capture nonstationarity of the emulator, which is of crucial importance in our application, as it will be demonstrated in the next section.

4. Numerical Results

We study here a challenging problem in which the fracture propagates vertically within a three-layered medium, as described schematically in (Fig.1). In this complex geological formation, the fracture growth tends to experiment a non-symmetric evolution due to abrupt changes in the confining stresses which assumes different values at each layer (Σ_0^1 for the layer 1, Σ_0^2 layer 2 and Σ_0^3 for layer 3). The layers are separated by interfaces χ_1 and χ_2, that the fracture will pass through at unknown injection times. In such a scenario, numerical simulations of the fracture propagation might help the operation in the field, trying to reduce the risks or to improve the stimulation. However, non accurate descriptions of the input parameters obtained by indirect measurements might hamper the ability of the numerical model to deliver trustworthy predictions. Here, we present a numerical modelling of HF, which also takes into account uncertainties inherited from imprecise measurement of rock properties. We combine the robust numerical method developed in (Peirce and Detourney, 2008); that

takes care of the deterministic aspects of the problem, with the MGPs described before. Those uncertainties are represented in the model by considering some of the input parameters as random variables. We elected the Elasticity Modulus and the confining stresses on each layer as those uncertain parameters. Indeed, those choices entails a reasonable first scenario to be analyzed, as those parameters have an important impact in the fracturing, and their values in the technical literature show a substantial dispersion that could be represented with the help of a probabilistic model.

The fracture takes place in a rocky medium consisting of three layers nominated hereafter as layer 1, layer2 and layer3. The fracture is initiated intermediary layer and evolves towards the other two. Taking in consideration typical values observed in this type of rock formation and with a volumetric injection rate $Q_0 = 0.11m^3/s$. We obtain the dimensionless values of the confining stress $\Sigma_0^1 = 1.25 \pm 0.02$, $\Sigma_0^2 = 1.41 \pm 0.041$, $\Sigma_0^3 = 1.45 \pm 0.031$. In the probabilistic model we consider that Σ_0^1, Σ_0^2, Σ_0^3 have a uniform distribution with mean $\overline{\Sigma_0^1}$=1.25, $\overline{\Sigma_0^2}$=1.41, $\overline{\Sigma_0^3}$=1.45 and the standard deviation $\sigma_{\Sigma_0^1}$=0.02, $\sigma_{\Sigma_0^2}$=0.041, $\sigma_{\Sigma_0^3}$=0.031. The Elasticity Modulus, also modeled as an uniform random variable, takes the following values: $\overline{G_E} = 1$ and σ_{G_E}=0.15. The quantities of interest directly computed from the simulation are: fracture length in upper and lower parts of the fracture $\ell_{up}(\tau, \varpi)$, $\ell_{low}(\tau, \varpi)$, the fracture aperture $\Omega(\chi, \tau, \varpi)$ and the fluid pressure $\Pi(\chi, \tau, \varpi)$ along the fracture.

The HF process begins at the initial time $\tau_0 = 11.72$ and stops at time $\tau_f = 240$. The interfaces are located at the position $\chi_1 = 4.2$ and $\chi_2 = -7.5$ with respect to the well position $\chi = 0$ (Fig.1). Using the expected value as nominal parameters, we simulate the fracture evolution and observe that the fracture reaches the interfaces 1 and 2 at the approximate time $\tau_{p1} = 100$ and $\tau_{p2} = 200$,respectively, as shown in (Fig.2). That figure also presents the fracture aperture evolution at the interfaces. In (Fig.2), we present the fracture length on both sides. We observe that the evolution of the length in the upper and lower is the symmetric until the fracture propagation reaches the first interface. When the fracture reaches the interface 2, the length of the fracture in the lower part feels this effect and changes its trend of growing abruptly. To have a better understanding of the nonlinearity and the non smoothness of HF response, we perform a sensitivity analysis by plotting outputs with respect to certain inputs. In this analysis, we consider outputs such as the upper lengths of the fracture in time τ $\ell_{up}(\tau = 47)$ and $\ell_{up}(\tau = 240)$, the fracture aperture at the interface χ_2, $\Omega(\chi_2, \tau = 240)$. These outputs are plotted with respect to the pair of inputs (Σ_0^3, G_E), (Σ_0^3, Σ_0^2). In (Figs. 3 - 4). Below, we will construct a surrogate to approximate efficiently the HF outputs having as inputs the four uncertain parameters, and we investigate its ability to handle the non smooth response reported in the previous figures.

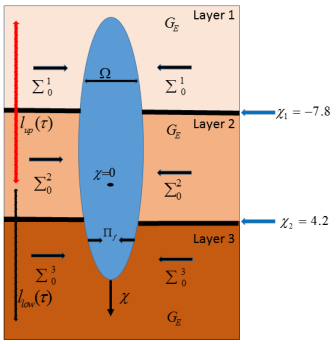

Figure 1: Schematic view of the layered medium

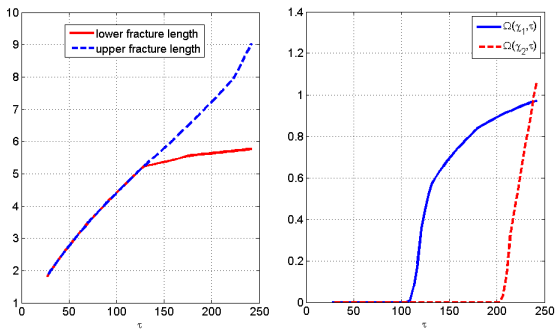

Figure 2: Fracture aperture at the interfaces evolution

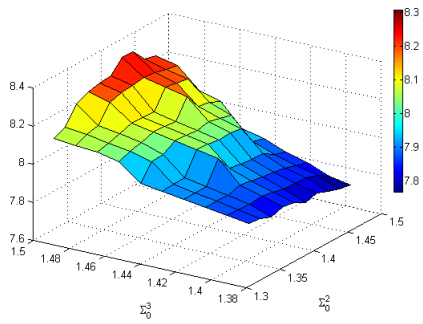

Figure 3: Fracture length $\ell_{up}(\tau = 47)$

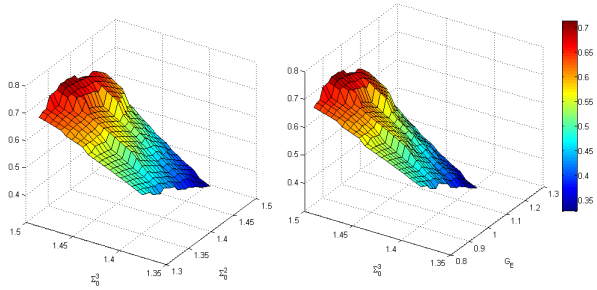

Figure 4: Fracture aperture $\Omega(\chi_2, \tau = 240)$

4.1. Surrogate computational performance

In order to assess the accuracy of the MGPs, we employ a reference solution obtained by Monte Carlo (MC) simulations. This reference solution is obtained after checking the convergence of some relevant outputs such as the final length of the fracture and the aperture at the interfaces positions depicted at (Figs. 5- 6). In these figures, we observed that 30,000 samples were enough for achieving an accurate approximation with the Monte Carlo method for the mean and variance of the outputs. Then, we verify the efficiency of the MGP surrogates by comparing its predictions with the ones provided by the MC simulations.

The surrogate depends on the definition of what inputs and outputs are relevant for a specific analysis. In a hydraulic fracture treatment, the final extension of the fracture and volume occupied by it make important quantities for the analysts. Although we are dealing with a dynamic scenario that develops in a spatial scenario, neither time or spatial positions were considered as inputs. We decided to have them only as indexes of the outputs in order to make the computational surrogate construction a tractable problem. We built the MGP electing as outputs the lower length of the fracture along the whole timeframe $\ell_{low}(\tau_0 : \tau_f)$, the fracture aperture after the fracture reaches the first layer. Therefore, in this particular application we have 4 inputs and a total of 108 outputs: $\{\ell_{low}(\tau_0 : \tau_f), \Omega(\chi_1, \tau_{p1} : \tau_f), \Omega(\chi_2, \tau_{p2} : \tau_f)\}$. We fixed the maximum number of training points in each stochastic element $N_{max} = 20$ and used with three different values of the accuracy threshold: $\delta = 10^{-3}, 10^{-4}, 10^{-5}$. In (Figs.7-8) we compare the results obtained with the surrogate with those computed with MC. The HF code was called 22; 34 and 99 times to construct the surrogate using the different levels of accuracy. We observe that the surrogate constructed with different values of δ have a mean value close to the reference solution (MC 30,000). The mean and standard deviation of outputs are close to the reference solution when $\delta = 10^{-5}$ correspond to 99 called of HF numerical code. These results show that, the efficiency of the MGP as surrogate in this example by achieving accuracy with a very low runs of the expensive original simulator.

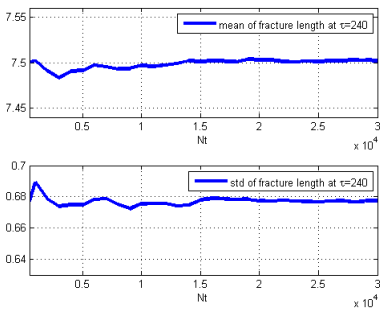

Figure 5: Convergence in mean and standard deviation of the the lower length of the fracture ℓ_{low} at $\tau = 240$ using MC

4.2. MGPs capturing local features of Hydraulic Fracture evolution

The objective of this section is to see how MGPs can cope with abrupt changes in the simulator response, like the ones featured in our previous sensitivity analysis that reveals different output behaviors for small changes in the input parameters. That

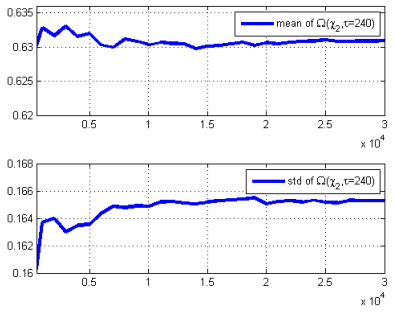

Figure 6: Convergence in mean and standard deviation of fracture aperture in the interface 2 $\Omega(\chi_2, \tau = 240)$ using MC

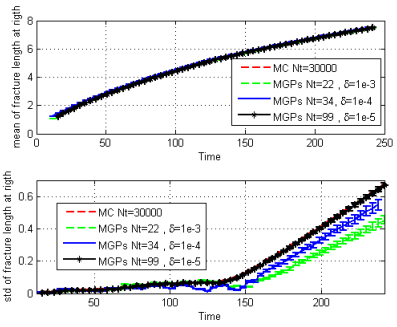

Figure 7: Fracture length mean and standard deviation MGP vs MC

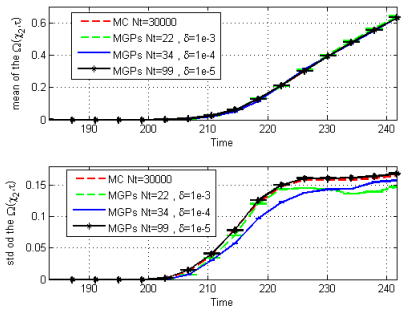

Figure 8: Fracture aperture $\Omega(\chi_2, \tau)$ mean and standard deviation MGP vs MC

can accommodate by dividing the input domain into subregions, such that inside each one the response is smooth. That is by far a non trivial task in the situation we are now analysing, as the abrupt changes in the response, are time dependent. To emphasize this, we construct two different surrogates. The surrogate 1 is built for describing the fracture evolution before it reaches the interfaces χ_1 or χ_2. The second one takes into consideration the whole timeframe of the evolution. The surrogate 1 is built using the outputs obtained at the injection time between $[\tau_0, \tau_p]$, such as the fracture length at lower and upper, the fracture aperture at the well and the aperture at the tips, $\{\ell_{up}(\tau_0 : \tau_{p1}), \ell_{low}(\tau_0 : \tau_{p1}), \Omega(\chi = 0, \tau p1), \Omega(\chi_{tip_r}, \tau_{p1}), \Omega(\chi_{tip_l}, \tau_{p1})\}$ with the total of M= 41 outputs, where $\tau_p < \tau_{p1} < \tau_{p2}$. The surrogate 2 is built using the outputs obtained at the injection interval $[\tau_{p1}, \tau_f]$. At these time. The surrogate 2 has as outputs $\{\ell_r(\tau_{p1} : \tau_f), \ell_l(\tau_{p2} : \tau_f), \Omega(\chi = 0, \tau_f), \Omega(\chi_{tip_r}, \tau_f), \Omega(\chi_{tip_l}, \tau_f)\}$ with a total of M= 46 outputs. The maximum number of training points was established as $N_{max} = 20$. The surrogates were constructed with the degree of prediction $\delta = 10^{-5}$. We observe that, to construct the surrogate 1 only two stochastic divisions (two local surrogates) were enough to get $\delta = 10^{-6}$ with the total of Nt=22 calls of the HF code . The surrogate 2 was constructed after 25 divisions of input space to get a $\delta = 10^{-5}$ with the total of Nt=296 calls of the HF code. The input domain decomposition is illustrated in in Fig.9. These results show the effects of the interfaces on the prediction of HF fracture statistics and the ability of MGPs to deal with this kind of challenge. When the fracture passes through the interfaces, the uncertainty in statistic prediction (error bars) becomes larger and does not satisfy the criterion of statistic prediction δ that was imposed. In this case, the MGPs refines the stochastic space adaptively to achieve the criterion that we impose, but still keeping the computational effort afordable.

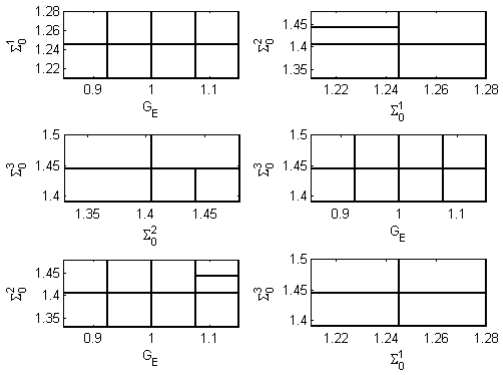

Figure 9: Final pairwise input space decomposition corresponding to the surrogate 2

4.3. Application in Uncertainty Quantification

A surrogate can be used for many different applications, such as optimization, uncertainty quantification, risk analysis, and global sensibility analysis. In the next subsection, we use surrogates constructed using MGPs to uncertainty quantification and risk analysis (George Shu Heng Pau, 2013).

In this section, we present the impact of uncertainties in HF evolution. The surrogates 2 obtained with $\delta = 10^{-4}$ is interrogated with 4000 samples to calculate the output statistics. In (Figs.10 - 11), we present the mean + uncertainty and the PDF of fracture aperture at the well and at the tips of fracture.

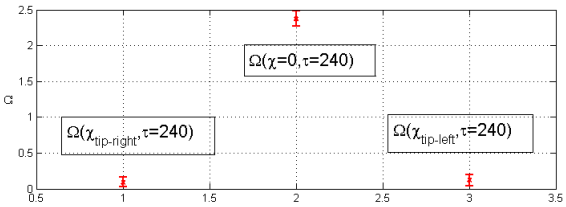

Figure 10: Mean + Uncertainty of fracture aperture Ω *at the well in tips right and left*

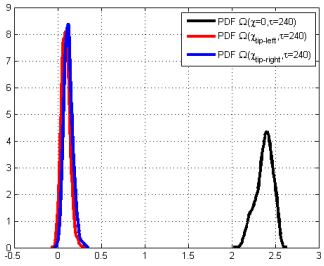

Figure 11: probability distribution function (PDF) of the aperture Ω *at the tips of the fracture at different times*

5. CONCLUSIONS

In this work, we show the efficiency of MGPs to approximate(surrogate) the nonlinear and nonsmooth behaviors of hydraulic fracture dynamics. The surrogate is used to compute the statistics of the response in the context of an Uncertainty Quantification analysis at a low computational cost when compared with the standard technique the Monte Carlo method. In the next future, we intend to employ MGPs as surrogates in the context of optimization of an HF process.

6. REFERENCES

Adachi, J. I. and Detournay, E. (2008). "Plane strain propagation of a hydraulic fracture in a permeable rock." *Engineering Fracture Mechanics*, 4666–4694.

Bilionis, I. and Zabaras, N. (2008). "Multi-output local gaussian process regression: Applications to uncertainty quantificaction." *Journal of Compuational Physics*.

George Shu Heng Pau, Y. Z. (2013). "Reduced order models for many-query subsurface flow applications." *Computational Geosciences, DOI 10.1007/s10596-013-9349-z*.

Ghanem, R. and Spanos, P. (1991). "Stochastic finite element method: A spectral approach." *Springer-Verlag*.

Mingjie Chen, Y. S. e. a. "Surrogate-based optimization of hydraulic fracturing in pre-existing fracture networks." *Computer and Geoscience*, 58, 69–79.

Peirce, A. (2014). "Modeling multi-scale processes in hydraulic fracture propagation using the implicit level set algorithm." *Department of Mathematics, University of British Columbia, Vancouver, British Columbia, V6T 1Z2, Canada*.

Peirce, A. and Detourney, E. (2008). "An implicit level set method for modeling hydraulically driven fractures." *Computer Methods in Applied Mechanics and Engineering 197, 2858-2885*.

Stefano Conti, A. O. (19 March 2010). "Bayesian emulation of complex multi-output and dynamic computer models." *Journal of Statistical Planning and Inference*, 140(3), 640–651.

Xiaoliang Wan, G. E. K. (2005). "An adaptive multi-element generalized polynomial chaos method for stochastic differential equations." *Journal of Computational Physics*.

Zio, S. and Rochinha, F. A. (2012). "A stochastic collocation approach for uncertainty quantification in hydraulic fracture numerical simulation." *International Journal for Uncertainty Quantification*, 145–160.